

# Adoptive Transfer of Immunomodulatory M2 Macrophages Prevents Type 1 Diabetes in NOD Mice

Roham Parsa,<sup>1</sup> Pernilla Andresen,<sup>1</sup> Alan Gillett,<sup>2</sup> Sohel Mia,<sup>1</sup> Xing-Mei Zhang,<sup>1</sup> Sofia Mayans,<sup>3</sup> Dan Holmberg,<sup>3</sup> and Robert A. Harris<sup>1</sup>

Macrophages are multifunctional immune cells that may either drive or modulate disease pathogenesis depending on their activation phenotype. Autoimmune type 1 diabetes (T1D) is a chronic proinflammatory condition characterized by unresolved destruction of pancreatic islets. Adoptive cell transfer of macrophages with immunosuppressive properties represents a novel immunotherapy for treatment of such chronic autoimmune diseases. We used a panel of cytokines and other stimuli to discern the most effective regimen for in vitro induction of immunosuppressive macrophages (M2r) and determined interleukin (IL)-4/IL-10/transforming growth factor- $\beta$  (TGF- $\beta$ ) to be optimal. M2r cells expressed programmed cell death 1 ligand-2, fragment crystallizable region  $\gamma$  receptor IIb, IL-10, and TGF- $\beta$ , had a potent deactivating effect on proinflammatory lipopolysaccharide/interferon- $\gamma$ -stimulated macrophages, and significantly suppressed T-cell proliferation. Clinical therapeutic efficacy was assessed after adoptive transfer in NOD T1D mice, and after a single transfer of M2r macrophages, >80% of treated NOD mice were protected against T1D for at least 3 months, even when transfer was conducted just prior to clinical onset. Fluorescent imaging analyses revealed that adoptively transferred M2r macrophages specifically homed to the inflamed pancreas, promoting  $\beta$ -cell survival. We suggest that M2r macrophage therapy represents a novel intervention that stops ongoing autoimmune T1D and may have relevance in a clinical setting. *Diabetes* 61:2881–2892, 2012

**M**acrophages have critical functions in both innate and adaptive immune responses. They are present in almost every tissue, recognize exogenous/endogenous danger signals through pattern-recognition receptors, produce various cytokines/chemokines that orchestrate immune responses at the site of inflammation, and function as professional antigen-presenting cells (APCs).

Two macrophage activation states have been defined in rodents and humans: “classically activated” (M1) cells have proinflammatory effector functions, and “alternatively activated” (M2) cells have anti-inflammatory properties. The existence of these different activation states implies prominent roles in different phases of an immunological

response, i.e., inflammation versus resolution and tissue remodeling. M1 cells are identified by high expression of the enzyme inducible nitric oxide (NO) synthase, a potent respiratory burst, and secretion of proinflammatory cytokines such as tumor necrosis factor- $\alpha$  (TNF- $\alpha$ ) and interleukin (IL)-12. The activation is induced by two signals, one toll-like receptor agonist, such as lipopolysaccharide (LPS), and one cytokine receptor-mediated signal, e.g., interferon- $\gamma$  (IFN- $\gamma$ ) (1,2).

We now understand that there are subpopulations of M2 macrophages, different types of activation leading to different functional phenotypes. M2 cells are generally characterized by secretion of anti-inflammatory cytokines such as IL-10 and by low or no secretion of proinflammatory cytokines. IL-4 was initially identified as an inducer of M2 macrophages (3), and it was later discerned that IL-4, in combination with IL-13, enhanced induction of wound-healing macrophages (M2a) (4). Further investigations determined that stimulation with glucocorticoids (e.g., dexamethasone), IL-10, immune complexes in combination with toll-like receptor agonists, and transforming growth factor- $\beta$  (TGF- $\beta$ ) could induce at least two further distinct M2 polarization states with immunoregulatory properties (M2b and M2c) (1,5). We have previously studied macrophage phenotypes from autoimmune-resistant and -susceptible rodent strains and have determined that there is a diversity of M1 activation phenotypes; autoimmune-susceptible strains have a common phenotype that contributes to prolongation of inflammation instead of its resolution (6). Similar genetically determined aberrant macrophage phenotypes have also been reported for NOD mice (7,8) and in human type 1 diabetes (T1D) (9,10). This indicates that there is a genetic predisposition for autoimmune susceptibility regarding macrophage phenotype and implies that individuals with autoimmune diseases may lack the ability to generate a cellular phenotype important in the resolution of inflammation.

Evidence of “immune regulatory” macrophage activity derives from cancer models in which tumor-associated macrophages have been reported to both suppress tumor immunity and promote tumor survival (5). Several in vitro (11,12) and in vivo disease studies (13–16) have investigated the regulatory role of macrophages in suppressing inflammation, the latter including models of multiple sclerosis, kidney disease, and spinal cord injury. Although these findings clearly indicate the important role of macrophages in the resolution of inflammation, there is no definitive consensus about their mechanism of action or optimal protocols for their induction.

T1D is an autoimmune disease in which insulin-producing  $\beta$ -cells in the pancreas are attacked by leukocytes (macrophages and cluster of differentiation [CD]4<sup>+</sup> and CD8<sup>+</sup> T cells) (17), which leads to a subsequent loss of glucose control and acute complications. The most widely used

From <sup>1</sup>Applied Immunology, Center for Molecular Medicine, Karolinska University Hospital at Solna, Department of Clinical Neuroscience, Karolinska Institutet, Stockholm, Sweden; <sup>2</sup>Neuroimmunology, Center for Molecular Medicine, Karolinska University Hospital at Solna, Department of Clinical Neuroscience, Karolinska Institutet, Stockholm, Sweden; and the <sup>3</sup>Department of Medical Biosciences, Umeå University, Umeå, Sweden.

Corresponding author: Robert A. Harris, robert.harris@ki.se.

Received 23 November 2011 and accepted 3 May 2012.

DOI: 10.2337/db11-1635

This article contains Supplementary Data online at <http://diabetes.diabetesjournals.org/lookup/suppl/doi:10.2337/db11-1635/-/DC1>.

A.G., S.Mi., and X.-M.Z. contributed equally to this study.

© 2012 by the American Diabetes Association. Readers may use this article as long as the work is properly cited, the use is educational and not for profit, and the work is not altered. See <http://creativecommons.org/licenses/by-nc-nd/3.0/> for details.

animal model for investigation of T1D is the NOD mouse (18) in which diabetes spontaneously develops between 12 and 30 weeks of age after initial leukocyte infiltration into the pancreas (insulinitis) between 3 and 5 weeks of age. Macrophages have been demonstrated to have a prominent role in T1D pathogenesis (19). Early M1 macrophage infiltration induces  $\beta$ -cell death and activates cytotoxic CD8<sup>+</sup> T cells (20,21). Although many studies have provided convincing evidence of the destructive role of M1 macrophages in T1D, it was recently reported that transgenic NOD mice that did not spontaneously develop T1D expressed M2 macrophage-associated genes in the pancreas (22), and that the 10–20% of NOD mice that do not develop T1D possess protective macrophages with a phagocytic/immunosuppressive phenotype (23).

Previous studies have investigated the use of cell transfer as an immunomodulatory therapy in NOD mice, with most reports using highly suppressive regulatory T cells (Tregs) (24,25). One drawback of this approach is that Treg antigen specificity is important for their suppressive ability (26), inferring that many Treg specificities might be required for the many pancreatic  $\beta$ -cell antigens implicated in T1D development. Adoptive cell transfer of tolerogenic dendritic cells has also been used in young NOD mice (5–8 weeks of age) during the early period of insulinitis (27). For an optimal effect in a clinical setting, it would be advantageous to use cell therapy at the clinical debut of disease.

The role of M2 macrophages in T1D and adoptive transfer of regulatory M2 macrophages as a cell therapy in T1D have never been reported before. In this study, we elucidated the ability of IL-4/IL-10/TGF- $\beta$  to induce an immunosuppressive M2 NOD macrophage phenotype (M2r). When M2r macrophages were adoptively transferred into late-stage pre-diabetic NOD mice, the onset of T1D was significantly reduced; advanced imaging analysis revealed protection of residual pancreatic islets concomitant with infiltration of the transferred M2r cells.

## RESEARCH DESIGN AND METHODS

**Animals.** The female NOD/ShiLtJ (NOD) and NOD/ShiLtJ-Tg(Foxp3-EGFP/cre)1cJbs (NOD-FoxP3-GFP) mice (The Jackson Laboratory, Bar Harbor, ME) and NOD.Cg-Tg(Tcr $\alpha$ BDC2.5, Ter $\beta$ BDC2.5)1Doi/DoiJ (NOD-BDC2.5) mice used (from Dr. P. Höglund, Karolinska Institutet) were between 7 and 12 weeks of age. Diabetes development was assessed through blood glucose measurements (Freestyle mini glucose reader; Abbott, Abbott Park, IL), with blood glucose levels >14.1 mmol/L (250 mg/dL) for two consecutive days in fed mice defining disease (Supplementary Fig. 1). All mice had initial fed blood glucose levels <8 mmol/L, and experiments were approved by the local ethics committee.

**Cell cultures.** Macrophages (98% purity) were obtained as described previously (28) using macrophage colony-stimulating factor-1-conditioned and endotoxin-free Dulbecco's modified Eagle's medium supplemented with 20% FBS (complete medium). Splenocytes and lymphocytes from lymph nodes were cocultured in 96-well, flat-bottom plates or 0.4- $\mu$ m transwell plates (Corning, Corning, NY) with 0.3  $\mu$ g/mL anti-CD3 molecular complex (BD) stimulation of T lymphocytes. Fixation of APCs with 0.5% paraformaldehyde (PFA) has been described previously (29). Depletion of Tregs (99.5% effective) was conducted using CD25 magnetic microbeads (Miltenyi Biotec) and isolation of naive T cells using CD4<sup>+</sup>CD62L<sup>+</sup> T-cell isolation kit II (Miltenyi Biotec). Proliferation of T cells was measured with [methyl-<sup>3</sup>H]thymidine (1  $\mu$ Ci/well; Amersham International, Amersham, U.K.). BDC2.5 T cells were stimulated with 500 ng/mL mimotope 1040-31 peptide (Anaspec, Fremont, CA).

**Reagents.** Final concentrations were applied as follows: 50 ng/mL LPS, 200 nM dexamethasone (Sigma-Aldrich), 50 ng/mL vitamin D<sub>3</sub> (Merck, Rahway, NJ), and 20 ng/mL recombinant mouse IL-4, IL-10, IL-13, and IFN- $\gamma$  and recombinant human TGF- $\beta$ 1 (R&D Systems, Minneapolis, MN). Carboxyfluorescein succinimidyl ester (CFSE) (5–10  $\mu$ M; Invitrogen) was used for measuring proliferation. Antibodies against CD86 (GL1), programmed cell death 1 ligand-1 (PD-L1) (MIH5), PD-L2 (TY25; all eBioscience), CD3 $\epsilon$  (500A2; BD), CD3 (17A2; Biolegend, San Diego, CA), CD4 (GK1.5), CD8 $\alpha$  (53-6.7), CD62L (MEL-14; all Beckman Coulter), and CD44 (IM7; BD) and isotype control rat IgG2a

(eBioscience) and IgG2b (eBioscience) were used for flow cytometric analyses. Dextran Alexa Fluor 647 (10,000 MW; Invitrogen) was used for endocytosis. Samples were run in a Gallios flow cytometer (Beckman Coulter, Brea, CA) and analyzed with Kaluza v1.1 (Beckman Coulter) and FlowJo v7.6.1 (Tree Star, Ashland, OR) software.

**Cytokine analyses.** ELISA kits were used for detection of secreted TNF, IL-6, TGF- $\beta$ , and IL-10 in cell culture supernatants (Biolegend and R&D Systems).

**NO detection.** NO activity was measured as nitrite in macrophage cell culture supernatants using the Griess reagent (Sigma-Aldrich) and measuring absorbance at 540 nm.

**Taqman low-density arrays.** RNA was extracted from stimulated macrophages ( $1 \times 10^6$  cells/mL) using the RNeasy kit (Qiagen, Inc.), and RNA concentrations were measured by spectroscopy (NanoDrop, Rockland, DE). cDNA was synthesized using SUPERScript II reverse transcriptase (Invitrogen). Data were analyzed using the comparative cycle threshold method and normalized using the geometric mean of two housekeeping genes (glyceraldehyde-3-phosphate dehydrogenase and hypoxanthine-guanine phosphoribosyltransferase). All experiments were related to untreated macrophage control.

**Macrophage adoptive transfer.** Macrophages stimulated with IL-4/IL-10/TGF- $\beta$  for 24 h or untreated macrophages (cultured in medium alone) were injected intraperitoneally with PBS as vehicle into groups of 8–12 mice at doses based on our previous studies (30).

**Optical projection tomography.** Dorsal pancreata from perfused and 4% PFA-fixed mice were dissected and stored in PFA for 30–60 min at 4°C before stepwise transfer to 100% methanol and storage at –20°C. Staining for insulin and CD3 using whole-mount immunofluorescence and optical projection tomography scanning protocols were performed as previously described (31). The generation of tomographic reconstructions, images, and movies was performed as previously described (32) using the program NRecon v1.5.0 (SkyScan, Kontich, Belgium) visualization software module for Volocity v5.2.1 (Improvision; PerkinElmer, Waltham, MA).

**Immunohistopathology.** Isoflurane-killed mice were perfused first with PBS and then fixed with 4% PFA, after which dorsal pancreata were isolated and prepared for cryosectioning. Transverse cryosections (14  $\mu$ m) (Microm cryostat-microtome, Heidelberg, Germany) were mounted on glass slides and stored at –20°C. Staining comprised blocking of nonspecific binding with 5% goat serum/PBS/0.3% Triton X-100/0.01% sodium azide (Sigma-Aldrich) for 30 min, incubation with primary antibodies (guinea pig polyclonal anti-insulin [1:100; Abcam]; rat anti-mouse CD3 molecule complex [1:50; BD]) overnight at 4°C and then for 1 h at room temperature with the respective goat anti-guinea pig Alexa Fluor 594 and goat anti-rat Alexa Fluor 488 (both 1:200; Molecular Probes) secondary antibodies. Sections were counterstained with DAPI and analyzed using a Leica DRMBE fluorescent microscope with DeltaPix software. Two to five slides per mouse were analyzed when insulin-positive islets were counted. Mean values are presented.

**In vivo macrophage tracking.** M2r macrophages and untreated macrophages were incubated for 5 min at 37°C with 3.5  $\mu$ g/mL XenoLight DiR (1,1'-dioctadecyl-3,3,3',3'-tetramethylindotricarbocyanine iodide Caliper Life Sciences, Hopkinton, MA), DiI (1,1'-dioctadecyl-3,3,3',3'-tetramethylindocarbocyanine perchlorate), or DiD (1,1'-dioctadecyl-3,3,3',3'-tetramethylindocarbocyanine perchlorate; Invitrogen) prior to intraperitoneal injection. Mice were anesthetized and imaged using IVIS Spectrum (Caliper Life Sciences) with ex.710/em.760 filters for DiR. Images were analyzed with Living Image v3.2 (Caliper Life Sciences) software. Emission from control organs was subtracted from DiR cell-treated organs when quantification of macrophage migration was made. Retrieval of adoptively transferred macrophages from pancreata and pancreatic lymph nodes (PLNs) was conducted by enzymatic digestion with liberase, DNase (Roche), and hyaluronidase (Sigma-Aldrich). Debri and exocrine/endocrine cells were removed using M-Lympholyte (Cedarlane, Burlington, Ontario, Canada) phase separation.

**Statistical analysis.** Statistical significance was determined by Mann-Whitney *U* test (GraphPad software v5, San Diego, CA). A *P* value of <0.05 was considered significant, and error bars are presented in SEM.

## RESULTS

**Stimulation with IL-4, IL-10, and TGF- $\beta$  induces a distinct M2r phenotype.** We first screened a variety of stimulation protocols and characterized the induced M2 phenotypes. To assess the ability of different M2 stimuli to modulate the induction of proinflammatory M1 activation phenotypes, naive NOD macrophages were costimulated with LPS/IFN- $\gamma$  (M1) and each M2-inducing stimulus, alone or in different combinations. NO levels were significantly reduced by the synergistic effect of TGF- $\beta$  and

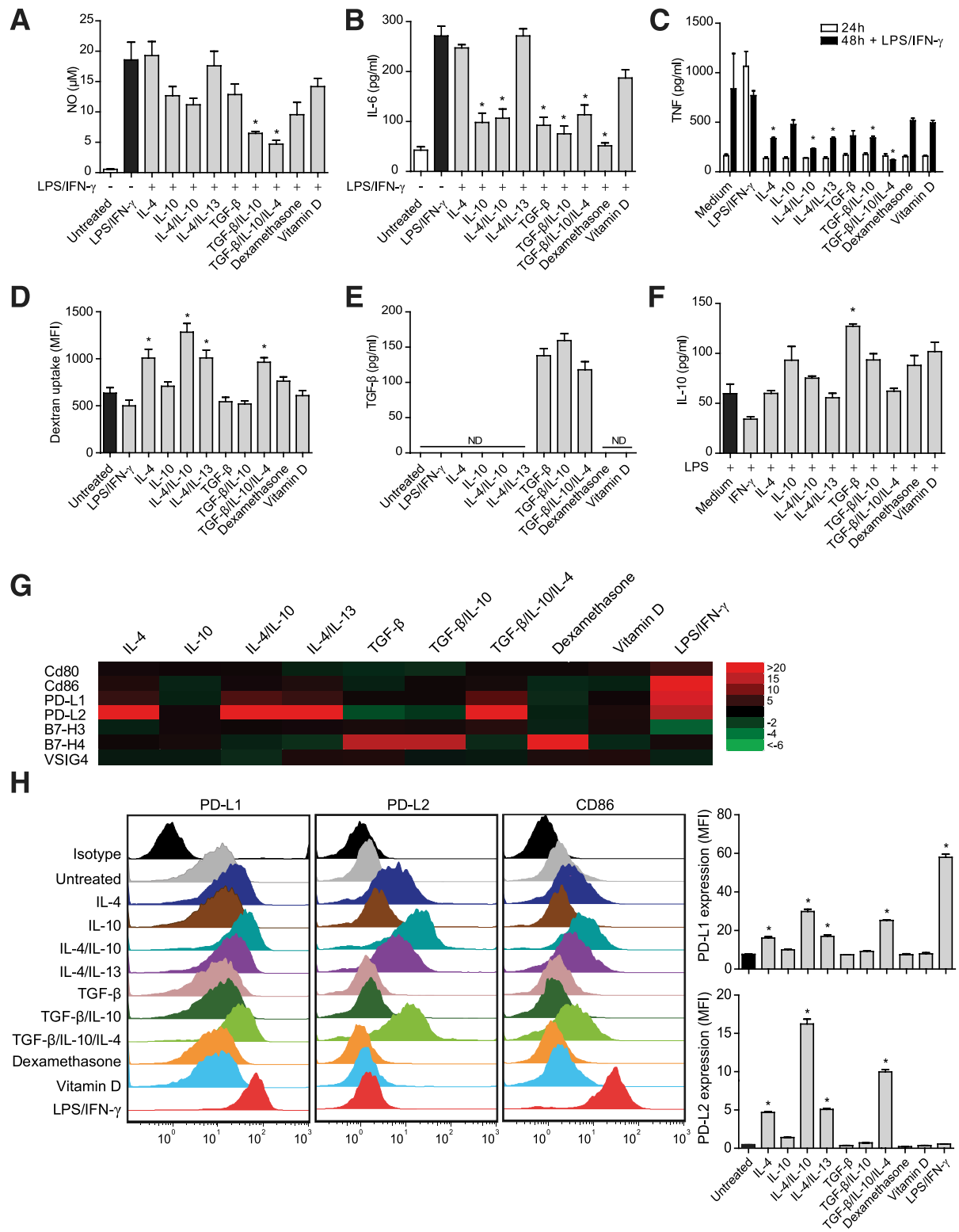


**FIG. 1.** IL-4, IL-10, and TGF- $\beta$  induce a distinct anti-inflammatory M2 phenotype. Macrophages ( $1 \times 10^5$ ) were costimulated for 72 h with the respective stimulus and LPS/IFN- $\gamma$  to determine levels of the proinflammatory mediators NO (A) and IL-6 (B). C: TNF measurement after activation with the respective stimulus for 24 h followed by secondary stimulation with LPS/IFN- $\gamma$  for 24 h (48 h). D: Endocytosis assessed by stimulating  $5 \times 10^5$  macrophages for 24 h with the respective stimulus followed by 4 h incubation with Alexa Fluor 647-coupled dextran. Bars represent mean fluorescence intensity (MFI). E: Levels of biologically active TGF- $\beta$  secretion in  $5 \times 10^5$  macrophages stimulated for 1 h, followed by 24 h incubation in fresh complete medium. F: IL-10 after costimulation of  $5 \times 10^5$  macrophages for 1 h with the described stimulus and LPS, and further incubation in fresh complete medium for 24 h. G: Gene expression of costimulatory molecules identified using low-density arrays. Color patterns visualize fold gene expression relative to untreated controls (red indicates increase, green indicates decrease, and black designates no fold difference). H: PD-L1, PD-L2, and CD86 receptor expressions analyzed by flow cytometry (MFI) using receptor-specific antibody staining. Each color represents one macrophage stimulation (24 h) regimen. All results are representative of three independent experiments. Statistical comparisons were conducted against LPS/IFN- $\gamma$  (A and B) or untreated (C–H) controls (black bars;  $n = 4$ ). White bars represent negative controls. ND, not detectable. Error bars are presented in SEM. \* $P < 0.05$ .

IL-10 (Fig. 1A). Addition of IL-10 or TGF- $\beta$  had significant downregulatory effects on IL-6 (Fig. 1B) and TNF (data not included) production compared with the LPS/IFN- $\gamma$  control. The triple combination of IL-4/IL-10/TGF- $\beta$  downregulated production of all three of these proinflammatory molecules.

To assess the fate of M2 phenotypes after secondary proinflammatory stimulation, macrophages were first M2 induced for 24 h, supernatants were washed away, and medium containing supplemented LPS/IFN- $\gamma$  was added for another 24 h. Resultant proinflammatory TNF levels were significantly lower from the M2 cells initially activated by IL-4/IL-10/TGF- $\beta$  (Fig. 1C).

Endocytosis is an important function during inflammation for clearance of both apoptotic cells and cellular debris from the local environment. The endocytic potential of induced M2 macrophages was assessed by uptake of fluorescently labeled dextran, and we determined that IL-4, either alone or in combination, induces enhanced endocytic activity in NOD macrophages (Fig. 1D).

As IL-10 and TGF- $\beta$  both have deactivating effects on macrophages and are important during the resolution of inflammation (33–35), we next investigated if the M2 induction protocols led to their secretion by macrophages. Relatively high levels of biologically active TGF- $\beta$  (Fig. 1E) were detected in macrophages that had been stimulated for only 1 h with TGF- $\beta$  itself. The significant induction of IL-10 protein required TGF- $\beta$  stimulation and concomitant activation with LPS (Fig. 1F), as previously reported (36). As LPS is proinflammatory, we also measured TNF in this setting and confirmed that the triple combination of IL-4/IL-10/TGF- $\beta$  resulted in significantly lower levels of TNF (data not included).

Taken together, the findings of this screening of M2 induction protocols indicate that the triple combination of IL-4/IL-10/TGF- $\beta$  induces a specific M2r macrophage phenotype that partly derives from synergistic effects of the three inducing cytokines. Each cytokine contributes with specific features such as endocytosis, phenotype stability, and secretion of TGF- $\beta$  and IL-10.

**Differential expression of PD-L1/PD-L2 on M1/M2 macrophages.** A panel of B7 family (B7) costimulatory receptors, including CD80, CD86, B7-H3, B7-H4, V-set and Ig domain-containing 4 (VSI4) (B7S1), PD-L1, and PD-L2, were screened for expression, as they have documented abilities to promote either activation or inhibition of T cells (37). Our results demonstrate that these receptors are differentially expressed at both transcription (Fig. 1G) and protein (Fig. 1H) levels, depending on the stimulation protocol. In particular, PD-L1 and PD-L2 were differentially expressed, mainly due to the actions of LPS/IFN- $\gamma$  and IL-4, respectively. CD86 expression was strongly enhanced by LPS/IFN- $\gamma$ , but flow cytometry data revealed that IL-4 also induces minor expression of CD86 and PD-L1 (Fig. 1H). There were no major expression differences evident for CD80 or VSI4. Thus, the major finding was that elevated expression of PD-L1 in M1 macrophages and of PD-L2 in IL-4/IL-10/TGF- $\beta$ -induced M2r macrophages distinguished these different activation phenotypes.

Additional gene transcription phenotyping revealed an M2 signature (high expression of *Arg1*, *Ido1*, *Ido2*, and *Fcgr2b* and low expression of *Nos2*, *Th2 Ccl22*, and *Cxcl10*) (Fig. 2). IL-10 did not induce any major gene expression by itself but had a synergistic effect on IL-4-stimulated macrophages. **M2r macrophages retain an M2 signature after secondary proinflammatory stimulation both in vitro and in vivo.** To further assess the plasticity of M2r

macrophages, a set of experiments was performed (Fig. 3A). Preactivated (24 h) M2r macrophages were washed and stimulated with LPS/IFN- $\gamma$  for an additional 24 h before activation phenotyping (48 h). M2r macrophages significantly produced higher levels of IL-10 when stimulated with M1-inducing agents (Fig. 3B). PD-L2 expression was reduced after secondary stimulation but was still significantly higher relative to untreated (M0) and M1 control. CD86 was upregulated on M2r macrophages but still significantly lower than on M0 and M1 macrophages (Fig. 3C). To further characterize the resultant phenotype of secondary-activated M2r macrophages, a set of gene targets was analyzed using PCR. M2-specific gene transcripts of *Arg1*, *Tgfb1*, *Pdl2*, *Cd163*, *Fcgr2b*, *Ido1*, and *Mrc1* were still present in secondary LPS/IFN- $\gamma$ -stimulated M2r macrophages, but upregulation of M1-associated genes, such as *Pdl1*, *Cd86*, and *Nos2*, was also recorded (Fig. 3D). We additionally investigated the ex vivo phenotype of DiD-stained M2r macrophages in PLNs and pancreata from NOD-BDC2.5 mice 1 week after transfer (Fig. 3E). Around 78% of the DiD<sup>+</sup> M2r macrophages expressed PD-L2 before transfer, and ex vivo analysis of retrieved DiD<sup>+</sup>CD11b<sup>+</sup> M2r macrophages revealed that >50% still expressed PD-L2, although the majority of the transferred cells also coexpressed CD86 in the PLN. A similar scenario was evident in the pancreas but fewer M2r macrophages expressed PD-L2 (~42% in total). In summary, these data indicate that transferred M2r macrophages retain an M2 signature and do not adopt a dominant M1 phenotype on access of the inflamed pancreas.

**Adoptive cell transfer of M2r protects mice from T1D.** The cumulative in vitro data indicated that IL-4/IL-10/TGF- $\beta$  induced an optimal suppressive M2r macrophage phenotype. The in vivo immunoregulatory activity of these cells in a setting of autoimmune disease was next investigated through their adoptive intraperitoneal transfer into 16-week-old, prediabetic, NOD mice, a time point just prior to clinical onset. Strikingly, even at this late time of intervention, 83% of the M2r-treated mice (single treatment) were protected from T1D, whereas only 25% of mice injected with M0 macrophages or vehicle (PBS) were diabetes free after 3 months of follow-up (Fig. 4A). This result indicates the potent ability of M2r macrophages to halt an ongoing autoimmune disease process.

**M2r-treated mice exhibit preserved  $\beta$ -cell survival.** Given the impressive clinical effect of M2r therapy, the pancreata from M2r and M0 macrophage-treated mice were examined for endocrine and immune activities. After dissection at different time points, three-dimensional reconstructions of pancreata were performed using optical projection tomography (Fig. 4B and Supplementary Videos 1–5). Control mice at 16 weeks of age clearly had very active insulinitis and low numbers of insulin-positive islets (compared with 5-week-old NOD mice in which insulin-positive islets were abundant) (38). Conversely, a higher number of insulin-producing  $\beta$ -cells were detected in mice treated with M2r macrophages, indicating that transfer of M2r macrophages led to diminished  $\beta$ -cell destruction (Fig. 4B). Immunohistochemical analyses of pancreata revealed similar findings (Fig. 4C), with a modest, yet significant, quantifiable difference in pancreatic islet numbers in M2r-treated animals (Fig. 4D).

**Macrophages predominantly migrate to the pancreas/PLN.** Live cell tracking using the stable cell tracer DiR was used to study the fate of adoptively transferred macrophages

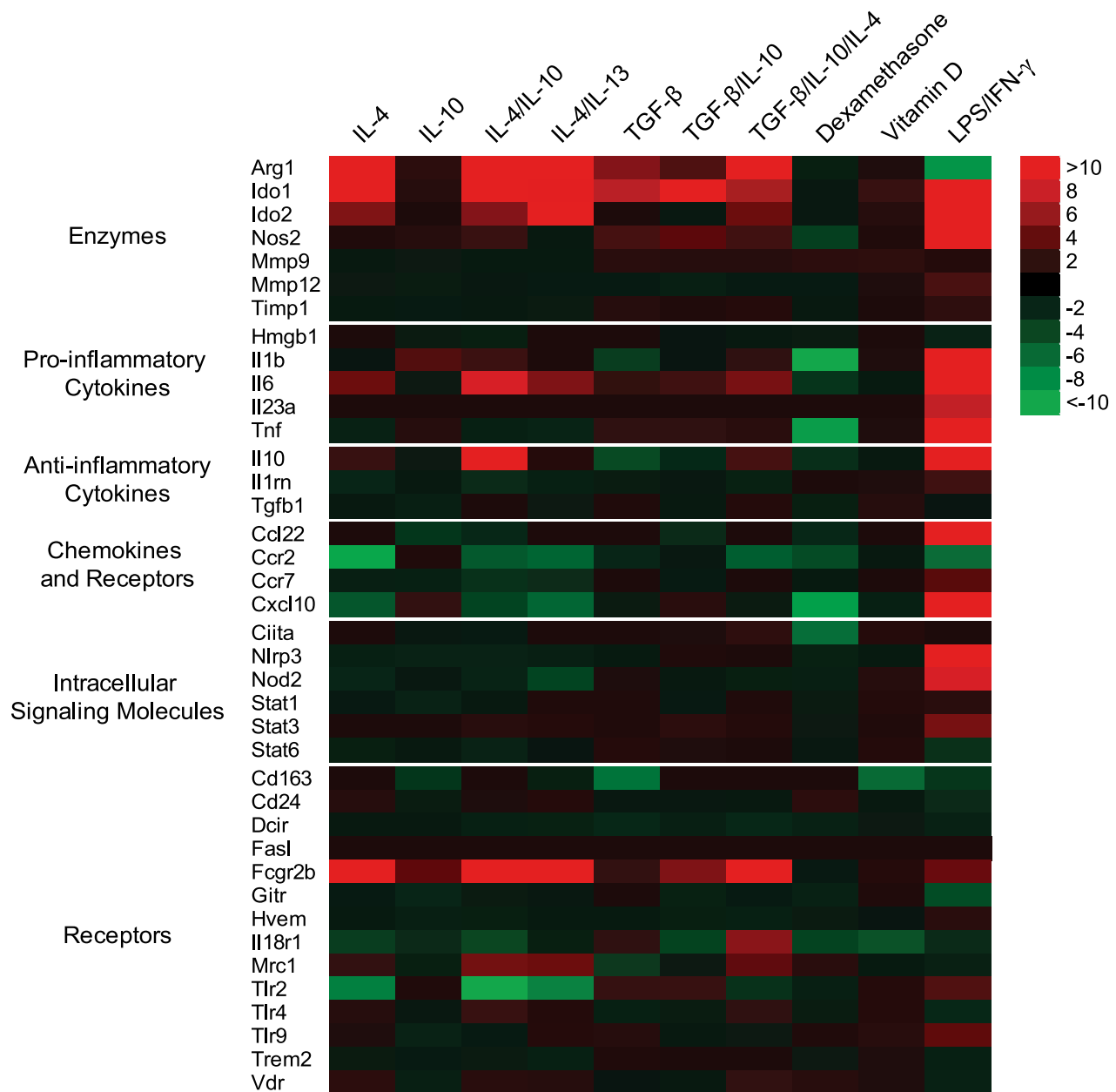


**FIG. 2. IL-4 dominantly regulates gene expression in 4 h-stimulated macrophages.** Color patterns visualize fold gene expression relative to untreated control. Red color indicates an increased fold expression and green color indicates a decreased fold expression. Black color designates no fold difference. Representative data from three individual animals.

into 10–12-week-old NOD mice. Macrophage migration was already evident 2 h postinjection; the cells were clustering near the pancreas and spleen (Fig. 5A), with no major differences between analyses on days 3, 6, and 8 postinjection, respectively. To confirm specific organ infiltration, organs were dissected out from mice on day 3 and analyzed individually (Fig. 5B). A significant majority of the fluorescent emissions from both M0 and M2r macrophages were localized to the pancreas and the PLN (Fig. 5C). Additional immunohistochemical analyses confirmed the presence of fluorescent M2r macrophages in close proximity to the remaining islets, with colocalization of CD11b immunostaining (day 3 depicted in Fig. 5D).

Taking these in vivo data together, we conclude that adoptively transferred M2r macrophages migrate to the

inflamed pancreas in NOD mice, resulting in protection from overt clinical T1D onset.

**M2r suppress T-cell proliferation in vivo.** To address the local in vivo mechanism of action of transferred M2r macrophages, NOD-BDC2.5 mice were used because the majority of their T cells recognize  $\beta$ -cell antigen. NOD-BDC2.5 mice were treated with M2r or M0 macrophages, PLNs were dissected out 1 week posttreatment, and antigen-specific proliferation was assessed in vitro. Lymphocytes from M2r-treated BDC2.5 mice proliferated less ( $16518 \pm 3,333$  counts per min [CPM]) than lymphocytes from M0-treated mice ( $32807 \pm 7,911$  CPM) upon restimulation with  $\beta$ -cell antigen peptide, clearly indicating immunomodulation of T cells by M2r macrophages in vivo (Fig. 6A). The relative numbers (percentage of cells and absolute numbers) of PLN CD4<sup>+</sup> and CD8<sup>+</sup> T-cell subsets were not affected by

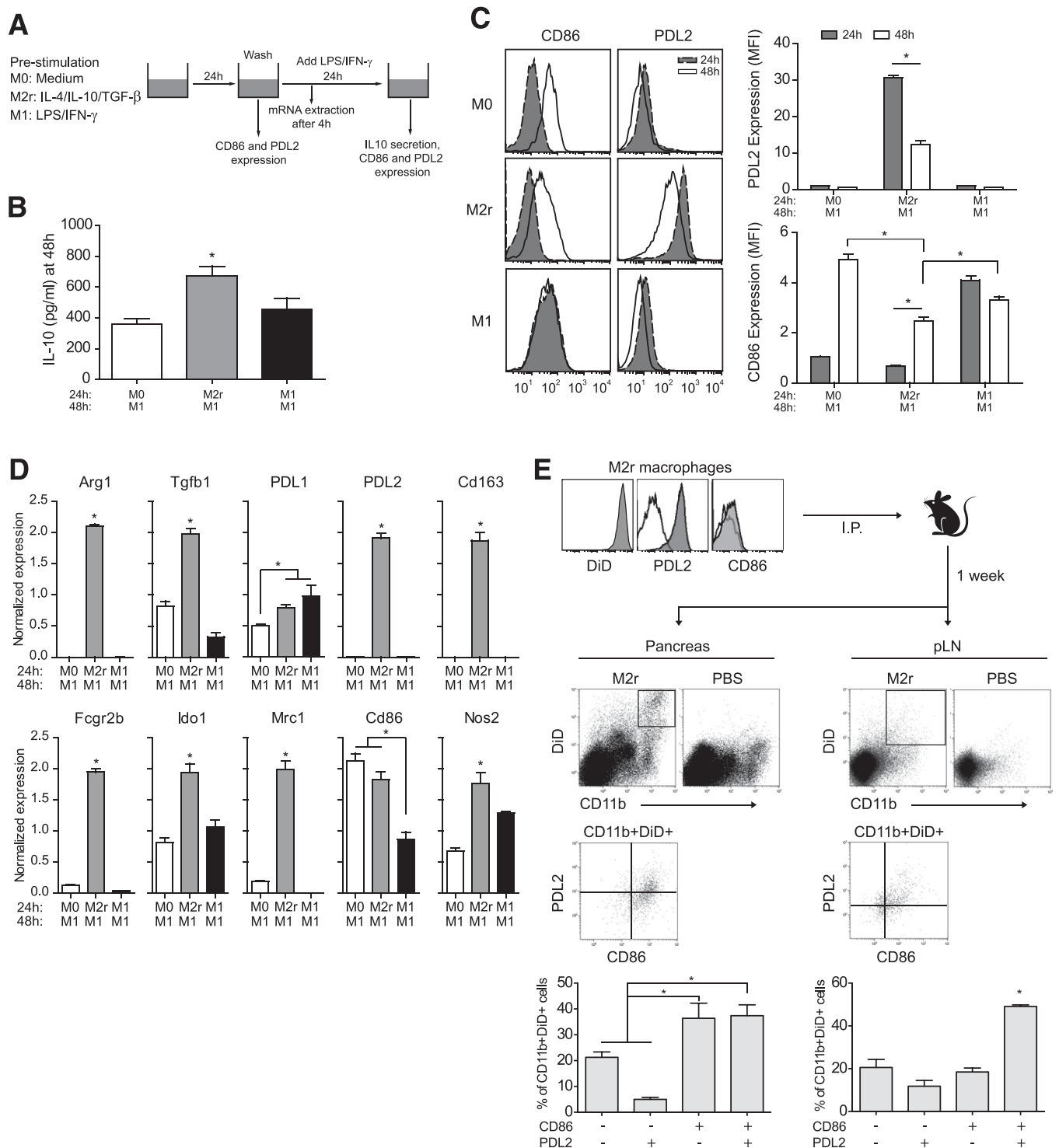


**FIG. 3.** M2r macrophages retain an M2 signature after secondary proinflammatory stimulation both in vitro and in vivo. **A:** Schematic experimental set-up. Primary activation with M0-, M2r-, or M1-inducing stimuli for 24 h, and secondary activation for an additional 24 h with LPS/IFN $\gamma$  (48 h). **B:** IL-10 production assessed by ELISA in secondary-activated macrophages. **C:** Flow cytometry analyses of CD86 and PD-L2 expression on primary- and secondary-activated macrophages. Histograms and mean fluorescence intensity analyses are depicted. MFI, mean fluorescence intensity. **D:** Selected gene expression assessed by RT-PCR after primary and secondary activations of macrophages. **E:** Ex vivo analyses of CD86 and PD-L2 on CD11b<sup>+</sup>DiD<sup>+</sup> macrophages recovered from pancreata (left) or PLNs (right). Histograms and percentage of cells depicted. The results are representative of two independent experiments ( $n = 4$ ). \* $P < 0.05$ .

M2r treatment (Fig. 6B). There was a trend ( $P = 0.06$ ) of altered activation state of these CD4<sup>+</sup> T cells in M2r-treated mice, as determined by CD62L and CD44 expression (Fig. 6C). Similar analyses of cells recovered from the pancreata of M2r-treated mice also revealed no differences

in T-cell subset compositions, although a trend ( $P = 0.06$ ) of lower CD8<sup>+</sup> T-cell activation was observed (Fig. 6D). These experiments were repeated in NOD-FoxP3-GFP mice. Again, there were no differences in the number of T-cell subsets or Tregs in PLNs from M2r-treated mice (Fig. 6E),

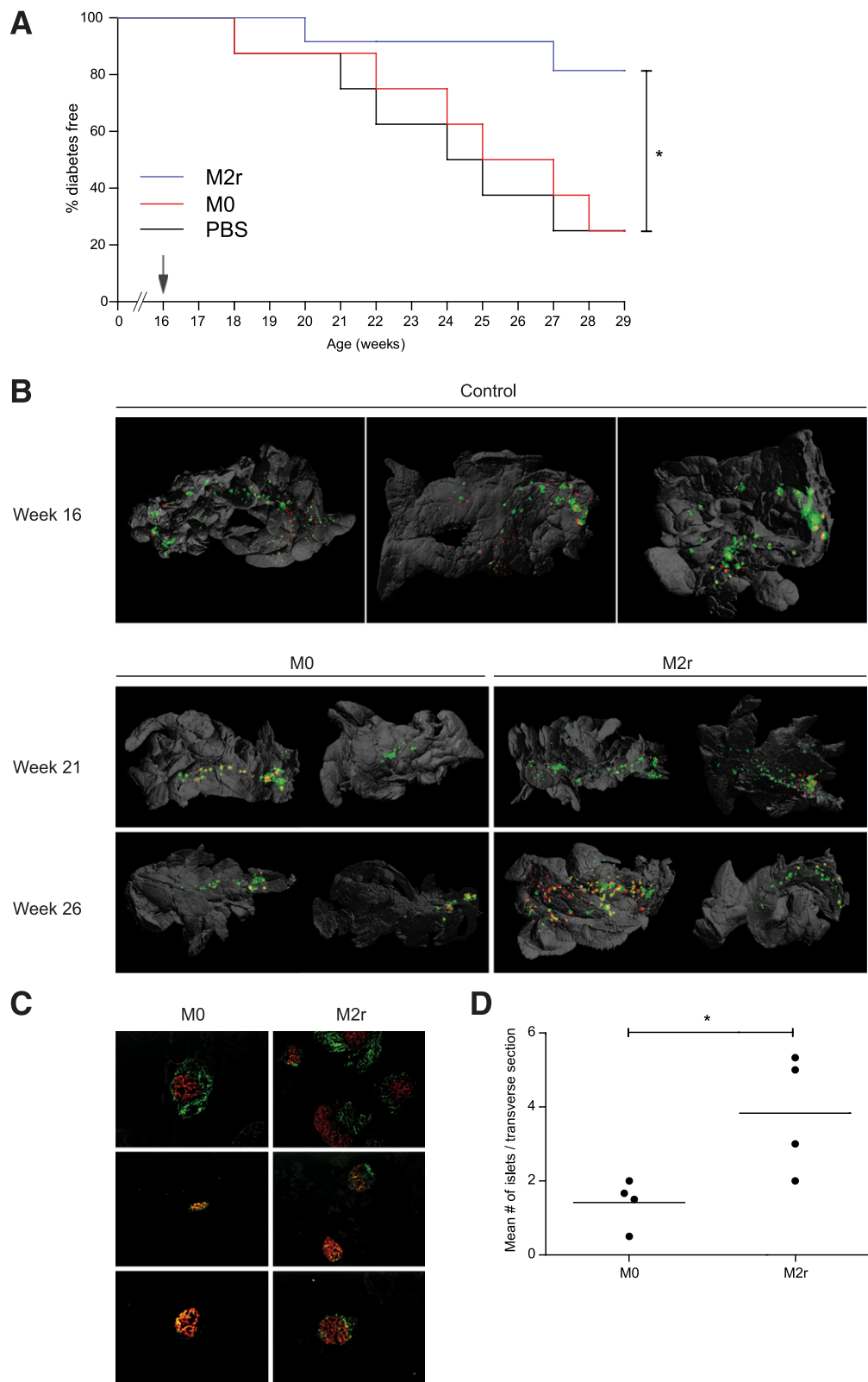


**FIG. 4.** M2r macrophages protect NOD mice from T1D by protecting pancreatic  $\beta$ -cells. **A:** IL-4/IL-10/TGF- $\beta$ -stimulated macrophages ( $2.5 \times 10^6$ ) (M2r, blue,  $n = 12$ ), untreated macrophages (M0, red,  $n = 8$ ), or vehicle (PBS, black,  $n = 8$ ) were intraperitoneally injected into 16-week-old prediabetic NOD mice (arrow). The M2r-treated group was significantly protected compared with M0 and PBS groups, as independently statistically analyzed using the Mantel-Cox test in a Kaplan-Meier survival graph. These results are representative data from two independent experiments with a similar outcome. **B:** Organs were stained with anti-insulin (red) and anti-CD3 (green)-specific antibodies prior to three-dimensional reconstruction using optical projection tomography. Yellow represents colocalization of CD3 and insulin staining, indicating insulinitis. Organs from 16-week-old mice represent three individual animals; 21- and 26-week-old organs represent two individual animals. **C:** After M2r or M0 macrophage transfer, pancreata were dissected 8 weeks later (24 weeks of age), and cryosections were stained with anti-insulin (red) and anti-CD3 (green) ( $n = 5$ ). **D:** Insulin<sup>+</sup> islets were counted manually from the sections in two to five transverse sections per animal to obtain the average number of insulin<sup>+</sup> islets per section ( $n = 4$ ). \* $P < 0.05$ . (A high-quality digital representation of this figure is available in the online issue.)

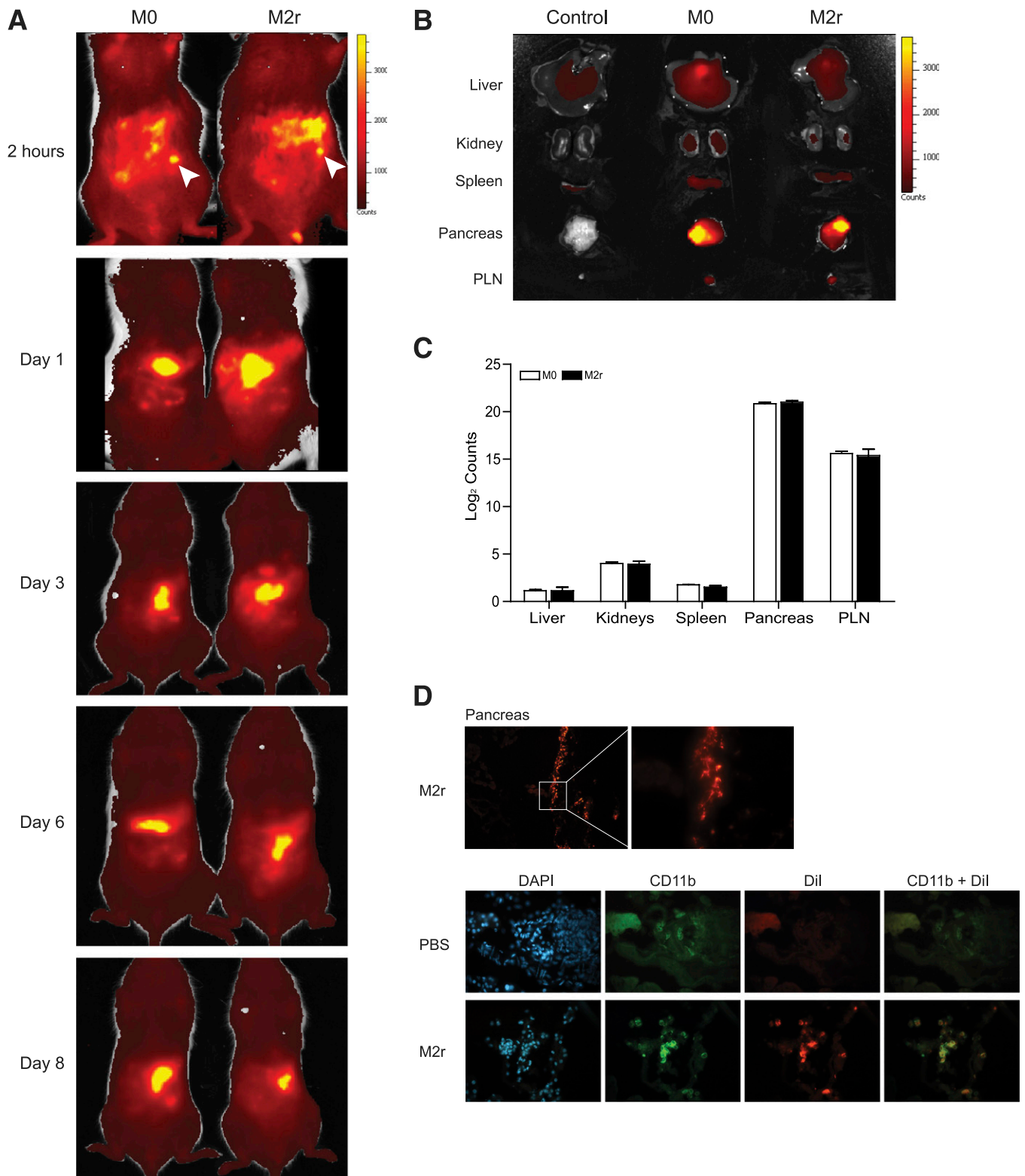


**FIG. 5.** Macrophages predominantly migrate to the pancreas and PLN. **A:** NOD mice (10–12 weeks of age) received  $3 \times 10^6$  DiI-labeled M2r or M0 macrophages intraperitoneally. Mice were anesthetized prior to anterior imaging after 2 h and 1, 3, 6, and 8 days post-macrophage injection. Bright yellow or dark red represents high or low photon counts, respectively, and white arrows indicate injection sites. Two individual mice were analyzed, and the data represent two individual experiments. **B:** After transfer, the liver, kidney, spleen, pancreas, and PLNs were dissected after 3 days post-macrophage injection. The image is representative of eight individual mice (four treated with M0 and four with M2r). **C:** Photon count from each organ in **B** was quantified, and control organ photon count was subtracted to obtain the real macrophage emission. Error bars are presented in SEM. **D:** NOD mice received  $2 \times 10^6$  DiI-labeled M2r macrophages (red) intraperitoneally, and pancreata were dissected at day 3 and stained for CD11b (green) and DAPI (blue). The data are representative of four different mice. (A high-quality digital representation of this figure is available in the online issue.)

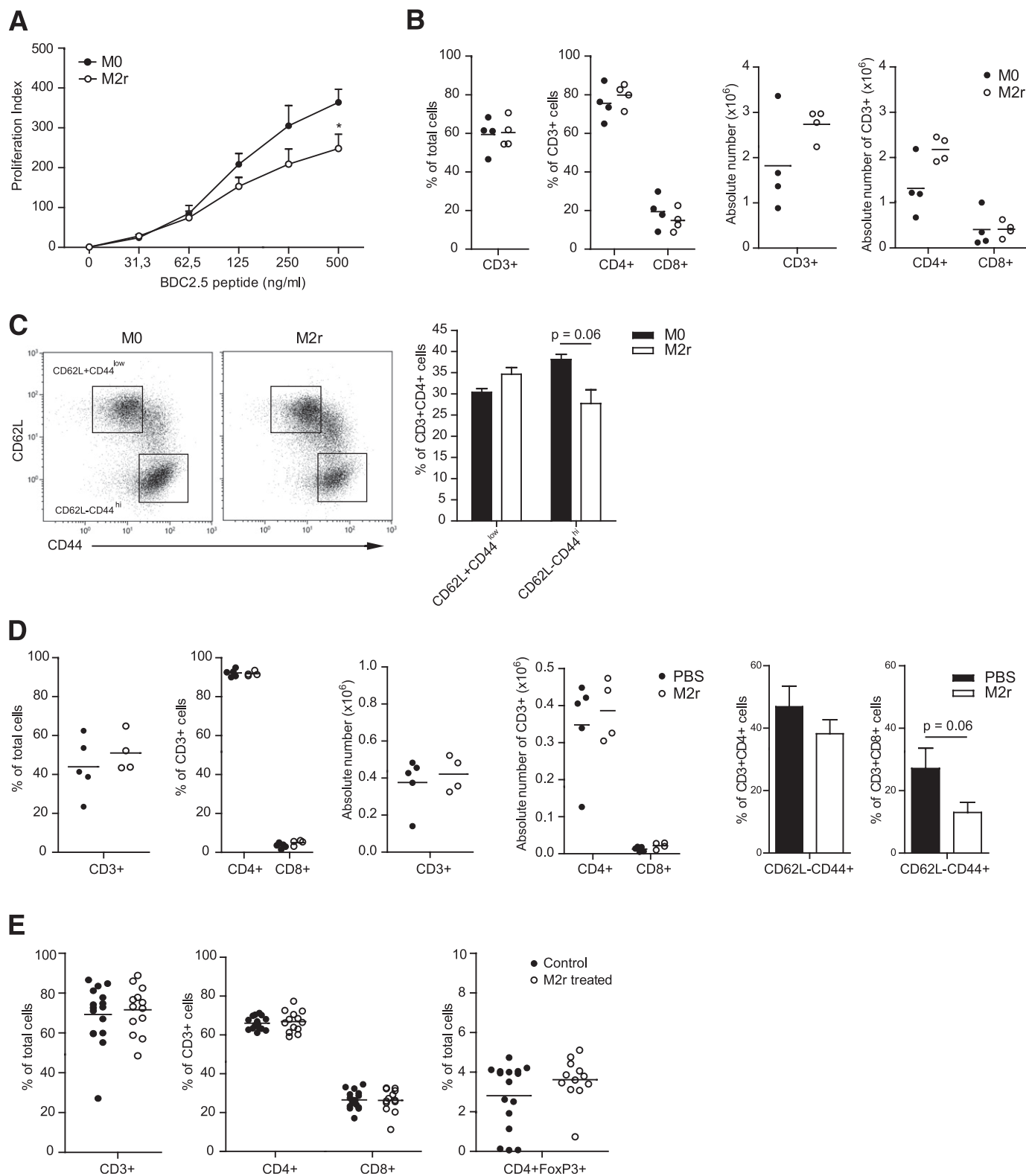


**FIG. 6.** M2r macrophages suppress ex vivo T-cell activity. M2r or M0 macrophages ( $2.5 \times 10^6$ ) were intraperitoneally injected into 12–16-week-old NOD-BDC2.5 mice. **A:** PLNs were dissected after 1 week, and lymphocytes were restimulated with BDC2.5 mimotope for 72 h to induce proliferation. Readout was CPM. **B:** PLNs were dissected after 1 week, and lymphocyte subsets were analyzed by flow cytometry for cell numbers (percent and absolute values). **C:** Activation status of CD4<sup>+</sup> subset assessed by CD44 and CD62L expression. **D:** Pancreata were dissected after 1 week, and lymphocyte subsets were analyzed by flow cytometry for cell numbers (percent and absolute values). **E:** M2r macrophages ( $2-3 \times 10^6$ ) or control (PBS) were intraperitoneally injected into 12–13-week-old NOD-FoxP3-GFP mice, PLNs were dissected after 1 week, and T-cell subset numbers were analyzed. The data from **A–D** represent two independent experiments ( $n = 4$ ). The data in **E** represent pooled data from four independent experiments. Error bars are presented in SEM. \* $P < 0.05$ .

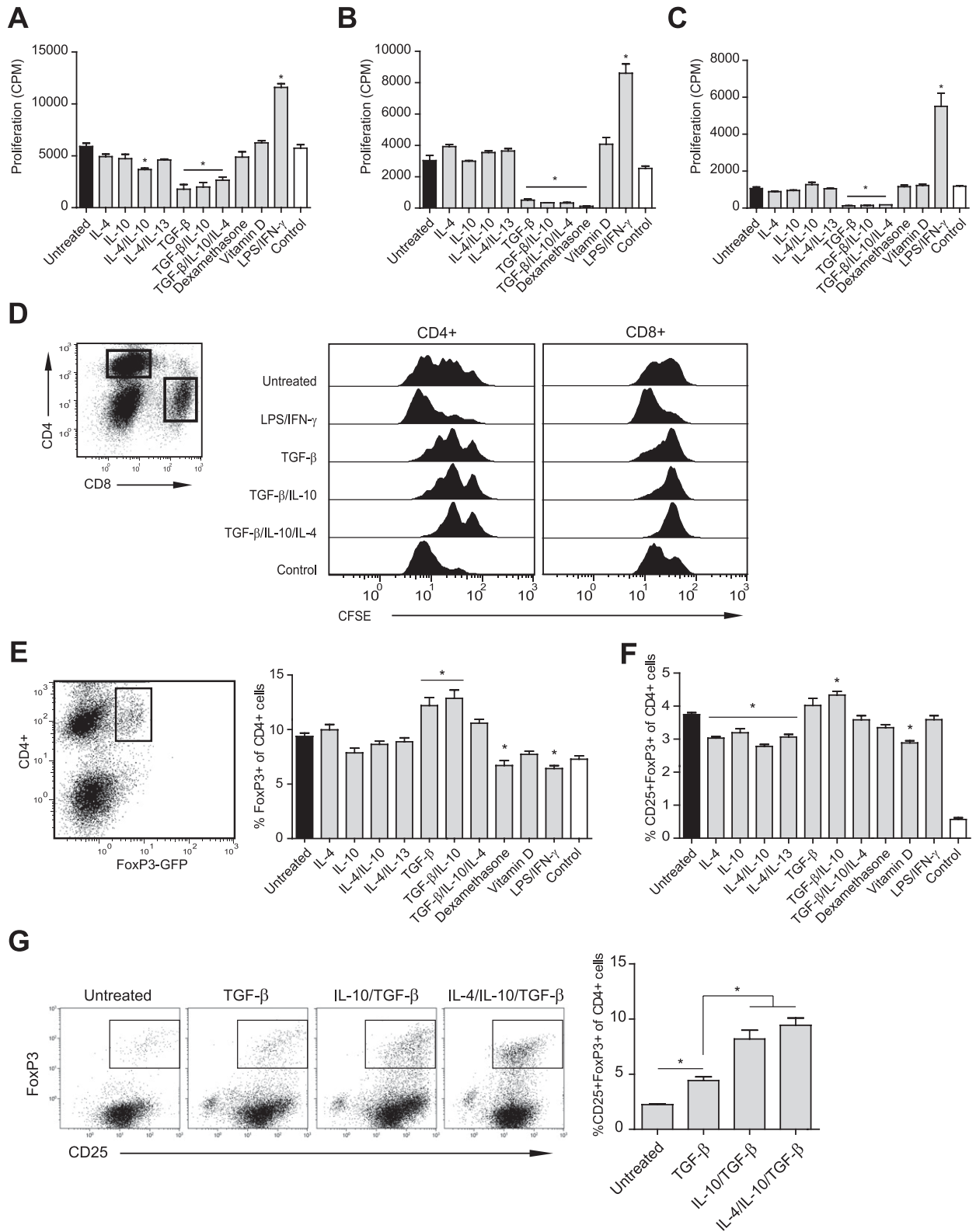


**FIG. 7.** TGF-β is important for M2 macrophages to suppress T-cell proliferation and the induction of Tregs in vitro. **A:** Suppression of T-cell proliferation (CPM) by stimulating  $25 \times 10^3$  macrophages for 24 h and further coculture with splenocytes and  $\alpha$ CD3 for 72 h. **B:** Macrophages ( $25 \times 10^3$ ) were cultured and stimulated for 24 h in a transwell upper chamber. Splenocytes and  $\alpha$ CD3 were added to the lower chamber, and cells were cocultured for 72 h and assessed for proliferation (CPM). **C:** Cell contact-dependent suppression of proliferation (CPM) evaluated by stimulating  $25 \times 10^3$  macrophages for 24 h followed by fixation and coculture with T cells, splenocytes, and  $\alpha$ CD3 for another 72 h. **D:** CFSE-stained splenocytes cocultured with  $25 \times 10^3$  pre-stimulated macrophages, as described above, for 96 h. Cells were either gated for CD4<sup>+</sup> or CD8<sup>+</sup> (left), and CFSE dilution was analyzed (right). **E:** Macrophages ( $25 \times 10^3$ ) were cultured and stimulated for 24 h before coculture with splenocytes from NOD-FoxP3-GFP mice for 96 h. Cells were gated for CD4<sup>+</sup> cells, and the percentage of GFP (FoxP3)-expressing cells was analyzed. **F:** Macrophages ( $25 \times 10^3$ ) were cultured with CD25<sup>+</sup>-depleted splenocytes from NOD-FoxP3-GFP mice for 96 h. Cells were gated for CD4<sup>+</sup> cells, and the percentage of CD25<sup>+</sup>GFP<sup>+</sup>-expressing cells was analyzed. **G:** Macrophages ( $25 \times 10^3$ ) were cultured with CD4<sup>+</sup>CD62L<sup>+</sup>CD25<sup>-</sup> T cells from NOD mice for 96 h. Cells were gated for CD4<sup>+</sup> cells, and the percentage of

nor were there major changes in T- or B-cell numbers detected in the spleen or other lymph nodes of treated NOD-FoxP3-GFP mice (data not included).

**TGF- $\beta$  has a major role in the suppressive and Treg induction activities of M2r macrophages.** Macrophage regulation of T-cell activities has been reported during the recent decade in both tumor and inflammation biology settings, but the nature of the cytokines that induce these suppressive abilities in macrophages is poorly understood. To confirm the *in vivo* findings of the suppressive action of M2r macrophages, an *in vitro* suppression assay was used, using anti-CD3 splenocyte activation. Optimization of cell densities led to the 1:16 (macrophage to T cell) ratio being selected for use in all further suppression assays (data not included). M2 induction by TGF- $\beta$ , either alone or in combination with IL-4/IL-10, was crucial for macrophage suppression of splenocyte proliferation (Fig. 7A). Both a transwell system and macrophage fixation were used in suppression assays to assess the relative contributions of cell contact-independent and -dependent suppressive mechanisms, respectively. TGF- $\beta$ -stimulated macrophages suppressed T-cell proliferation both in the transwell (Fig. 7B) and after fixation (Fig. 7C). Taken together, these results indicate that TGF- $\beta$  has an important role in the regulatory phenotype of macrophages to suppress T-cell activation mediated both by cell contact and via secreted factors. NOD splenocytes were also stained with carboxyfluorescein diacetate succinimidyl ester (CFSE) and cocultured with induced M2r macrophages, demonstrating that proliferation of both CD4<sup>+</sup> and CD8<sup>+</sup> T-cell subsets is suppressed (Fig. 7D).

When combined with IL-4/IL-10, TGF- $\beta$ -treated macrophages suppressed T-cell proliferation, secreted TGF- $\beta$ , and expressed PD-L2. As these represent molecules associated with Treg induction, the ability of M2 cells to induce Tregs was assessed *in vitro*. TGF- $\beta$  pretreatment of macrophages led to an increase in the percentage of Tregs induced from naive T cells *in vitro* (Fig. 7E). Interestingly, only TGF- $\beta$ /IL-10-stimulated macrophages had the ability to significantly induce Tregs from CD25<sup>+</sup>-depleted splenocytes (Fig. 7F). We additionally used naive CD4<sup>+</sup> T cells (CD62L<sup>+</sup>CD25<sup>-</sup>) to confirm that M2-stimulated macrophages induced Tregs (Fig. 7G).

## DISCUSSION

Macrophages are important in the pathogenesis of many autoimmune diseases, being the first cells to infiltrate the pancreata of NOD mice (39), major effector cells in experimental multiple sclerosis (40), and major TNF producers in rheumatoid arthritis (41). In contrast to the tissue-destructive functions of M1 macrophages in autoimmune diseases, the immunosuppressive and tolerogenic ability of M2 macrophages and dendritic cells has stimulated an emerging interest for these myeloid cells and their immunomodulatory roles in regulation of inflammation. The major finding of our current study is that a single adoptive transfer of *in vitro* induced immunosuppressive M2r macrophages can prevent imminent development of clinical T1D in NOD mice, illustrating the potential of this myeloid cell therapy to counteract an aggressive pathological process.

In screening to define an optimal suppressive macrophage activation phenotype *in vitro*, we applied an extensive panel

of activation protocols encompassing reported M2-inducing protocols. Taken together, these *in vitro* phenotypic analyses revealed that a spectrum of M2 phenotypes was induced via different induction protocols and that different readouts were required to distinguish these individual phenotypes. We finally selected the novel combination of IL-4/IL-10/TGF- $\beta$  for further study, a cytokine cocktail encompassing both M2a and M2c phenotypes (5) and indicating both potential regulatory and wound-healing functions of the induced M2r phenotype. Although PD-L1 and PD-L2 receptors have been discordantly reported as being either inhibitory of (42–44) or activating (45) coreceptors depending on the inflammatory scenario, we determined the expression signature of PD-L1<sup>low</sup>/PD-L2<sup>hi</sup>/CD86<sup>low</sup> in M2r cells, which contrasted with PD-L1<sup>hi</sup>/PD-L2<sup>neg</sup>/CD86<sup>hi</sup> expression in M1 cells.

The individual effects of IL-4, IL-10, and TGF- $\beta$  in the M2r induction protocol either synergized or antagonized expression of specific molecules, but this activation phenotype was functionally suppressive via both secreted and surface-expressed molecules. The production of both TGF- $\beta$  and IL-10 and low levels of TNF after co- or secondary stimulation with LPS clearly indicates their potential regulatory role. Functional analyses revealed that this novel anti-inflammatory phenotype could not only suppress T-cell proliferation *in vitro* but also modulate the *ex vivo* activation of PLN T cells. Considering that transferred M2r macrophages migrated to the inflamed pancreas, the deactivation of infiltrated proinflammatory macrophages, dendritic cells, or autoreactive T cells within the target organ could be one of the mechanisms explaining the clinical efficacy in preventing T1D development posttransfer into NOD mice, while they might also induce wound-healing processes in the target organ. Once in the proinflammatory environment of the pancreas, the transferred cells retained an M2 signature. The anti-inflammatory action of the M2r macrophages thus appears to be central to the clinical therapeutic effect, although the potential contribution of local *in vivo* Treg modulation cannot be ruled out.

We previously demonstrated an APC transfer therapy in a setting of experimental neuroinflammation (30) by adoptively transferring splenic major histocompatibility class II (MHCII<sup>+</sup>) cells into mice with previously induced encephalomyelitis and demonstrating a significant therapeutic effect of this cell therapy. During recent years, this has become an intense area of research, and other research groups have confirmed the therapeutic concept in both autoimmune neurologic and renal disease settings, indicating that the approach may be used in a variety of inflammatory settings. That T1D could be prevented by so late an intervention in NOD mice is striking and indicates both the potent immunosuppressive activity of the M2r phenotype and their novel role in T1D. Based on one injection, and in a nonantigen-dependent fashion, this cell therapy is clinically an attractive option for combining immunosuppressive and wound-healing activities.

## ACKNOWLEDGMENTS

This work was supported by grants from the Swedish Medical Research Council, Juvenile Diabetes Research Foundation, BarnDiabetes Fund, and Karolinska Institutet.

CD25<sup>+</sup>FoxP3<sup>+</sup>-expressing cells was analyzed. The results are representative of three independent (A–F) experiments and one experiment (G). Statistical comparison was conducted against untreated macrophage control (black bars;  $n = 4$ ). Control represents splenocytes without macrophages (white bars). Error bars are presented in SEM. \* $P < 0.05$ .

No potential conflicts of interest relevant to this article were reported.

R.P. designed the study, wrote the manuscript, and performed research. P.A., A.G., S.Mi., X.-M.Z., and S.Ma. performed research. D.H. designed the study and wrote the manuscript. R.A.H. designed and supervised the study and wrote the manuscript. All authors analyzed data and revised the manuscript. R.A.H. is the guarantor of this work and, as such, had full access to all the data in the study and takes responsibility for the integrity of the data and the accuracy of the data analysis.

The authors thank Dr. M. Jagodic and Dr. A. Ortlieb (Karolinska Institutet) for critical appraisal.

## REFERENCES

- Mosser DM, Edwards JP. Exploring the full spectrum of macrophage activation. *Nat Rev Immunol* 2008;8:958–969
- Mantovani A, Sica A, Sozzani S, Allavena P, Vecchi A, Locati M. The chemokine system in diverse forms of macrophage activation and polarization. *Trends Immunol* 2004;25:677–686
- Stein M, Keshav S, Harris N, Gordon S. Interleukin 4 potently enhances murine macrophage mannose receptor activity: a marker of alternative immunologic macrophage activation. *J Exp Med* 1992;176:287–292
- Gordon S. Alternative activation of macrophages. *Nat Rev Immunol* 2003;3:23–35
- Biswas SK, Mantovani A. Macrophage plasticity and interaction with lymphocyte subsets: cancer as a paradigm. *Nat Immunol* 2010;11:889–896
- Andersson A, Kokkola R, Wefer J, Erlandsson-Harris H, Harris RA. Differential macrophage expression of IL-12 and IL-23 upon innate immune activation defines rat autoimmune susceptibility. *J Leukoc Biol* 2004;76:1118–1124
- Alleva DG, Pavlovich RP, Grant C, Kaser SB, Beller DI. Aberrant macrophage cytokine production is a conserved feature among autoimmune-prone mouse strains: elevated interleukin (IL)-12 and an imbalance in tumor necrosis factor- $\alpha$  and IL-10 define a unique cytokine profile in macrophages from young nonobese diabetic mice. *Diabetes* 2000;49:1106–1115
- Marée AF, Komba M, Finegood DT, Edelstein-Keshet L. A quantitative comparison of rates of phagocytosis and digestion of apoptotic cells by macrophages from normal (BALB/c) and diabetes-prone (NOD) mice. *J Appl Physiol* 2008;104:157–169
- Plesner A, Greenbaum CJ, Gaur LK, Ernst RK, Lemmark A. Macrophages from high-risk HLA-DQB1\*0201/\*0302 type 1 diabetes mellitus patients are hypersensitive to lipopolysaccharide stimulation. *Scand J Immunol* 2002;56:522–529
- Stoffels K, Overbergh L, Giulietti A, et al. NOD macrophages produce high levels of inflammatory cytokines upon encounter of apoptotic or necrotic cells. *J Autoimmun* 2004;23:9–15
- Munn DH, Pressley J, Beall AC, Hudes R, Alderson MR. Selective activation-induced apoptosis of peripheral T cells imposed by macrophages. A potential mechanism of antigen-specific peripheral lymphocyte deletion. *J Immunol* 1996;156:523–532
- Savage ND, de Boer T, Walburg KV, et al. Human anti-inflammatory macrophages induce Foxp3+ GITR+ CD25+ regulatory T cells, which suppress via membrane-bound TGF $\beta$ 1. *J Immunol* 2008;181:2220–2226
- Weber MS, Prod'homme T, Youssef S, et al. Type II monocytes modulate T cell-mediated central nervous system autoimmune disease. *Nat Med* 2007;13:935–943
- Cao Q, Wang Y, Zheng D, et al. IL-10/TGF $\beta$ -modified macrophages induce regulatory T cells and protect against adriamycin nephrosis. *J Am Soc Nephrol* 2010;21:933–942
- Miyake Y, Asano K, Kaise H, Uemura M, Nakayama M, Tanaka M. Critical role of macrophages in the marginal zone in the suppression of immune responses to apoptotic cell-associated antigens. *J Clin Invest* 2007;117:2268–2278
- Shechter R, London A, Varol C, et al. Infiltrating blood-derived macrophages are vital cells playing an anti-inflammatory role in recovery from spinal cord injury in mice. *PLoS Med* 2009;6:e1000113
- Lehuen A, Diana J, Zaccone P, Cooke A. Immune cell crosstalk in type 1 diabetes. *Nat Rev Immunol* 2010;10:501–513
- Delovitch TL, Singh B. The nonobese diabetic mouse as a model of autoimmune diabetes: immune dysregulation gets the NOD. *Immunity* 1997;7:727–738
- Jun HS, Yoon CS, Zbytniuk L, van Rooijen N, Yoon JW. The role of macrophages in T cell-mediated autoimmune diabetes in nonobese diabetic mice. *J Exp Med* 1999;189:347–358
- Calderon B, Suri A, Unanue ER. In CD4+ T-cell-induced diabetes, macrophages are the final effector cells that mediate islet beta-cell killing: studies from an acute model. *Am J Pathol* 2006;169:2137–2147
- Jun HS, Santamaria P, Lim HW, Zhang ML, Yoon JW. Absolute requirement of macrophages for the development and activation of beta-cell cytotoxic CD8+ T-cells in T-cell receptor transgenic NOD mice. *Diabetes* 1999;48:34–42
- Calderon B, Suri A, Pan XO, Mills JC, Unanue ER. IFN- $\gamma$ -dependent regulatory circuits in immune inflammation highlighted in diabetes. *J Immunol* 2008;181:6964–6974
- Fu W, Wojtkiewicz G, Weissleder R, Benoist C, Mathis D. Early window of diabetes determinism in NOD mice, dependent on the complement receptor CR1g, identified by noninvasive imaging. *Nat Immunol* 2012;13:361–368
- Mukherjee R, Chaturvedi P, Qin HY, Singh B. CD4+CD25+ regulatory T cells generated in response to insulin B:9-23 peptide prevent adoptive transfer of diabetes by diabetogenic T cells. *J Autoimmun* 2003;21:221–237
- Roncarolo MG, Battaglia M. Regulatory T-cell immunotherapy for tolerance to self antigens and alloantigens in humans. *Nat Rev Immunol* 2007;7:585–598
- Tonkin DR, He J, Barbour G, Haskins K. Regulatory T cells prevent transfer of type 1 diabetes in NOD mice only when their antigen is present in vivo. *J Immunol* 2008;181:4516–4522
- Morin J, Faideau B, Gagnerault MC, Lepault F, Boitard C, Boudaly S. Passive transfer of fit-3L-derived dendritic cells delays diabetes development in NOD mice and associates with early production of interleukin (IL)-4 and IL-10 in the spleen of recipient mice. *Clin Exp Immunol* 2003;134:388–395
- Weischenfeldt J, Porse B. Bone Marrow-Derived Macrophages (BMM): isolation and applications. *CSH Protoc* 2008;2008.pdb.prot5080
- Harding CV, Ramachandra L. Presenting exogenous antigen to T cells. *Curr Protoc Immunol* 2010;Chapter 16:Unit 16.2
- Alanentalo T, Asayesh A, Morrison H, et al. Tomographic molecular imaging and 3D quantification within adult mouse organs. *Nat Methods* 2007;4:31–33
- Alanentalo T, Lorén CE, Larefalk A, Sharpe J, Holmberg D, Ahlgren U. High-resolution three-dimensional imaging of islet-infiltrate interactions based on optical projection tomography assessments of the intact adult mouse pancreas. *J Biomed Opt* 2008;13:054070
- Ouyang W, Rutz S, Crellin NK, Valdez PA, Hymowitz SG. Regulation and functions of the IL-10 family of cytokines in inflammation and disease. *Annu Rev Immunol* 2011;29:71–109
- Wan YY, Flavell RA. 'Yin-Yang' functions of transforming growth factor- $\beta$  and T regulatory cells in immune regulation. *Immunol Rev* 2007;220:199–213
- Saraiva M, O'Garra A. The regulation of IL-10 production by immune cells. *Nat Rev Immunol* 2010;10:170–181
- Maeda H, Kuwahara H, Ichimura Y, Ohtsuki M, Kurakata S, Shiraishi A. TGF- $\beta$  enhances macrophage ability to produce IL-10 in normal and tumor-bearing mice. *J Immunol* 1995;155:4926–4932
- Greenwald RJ, Freeman GJ, Sharpe AH. The B7 family revisited. *Annu Rev Immunol* 2005;23:515–548
- Alanentalo T, Hörnblad A, Mayans S, et al. Quantification and three-dimensional imaging of the insulinitis-induced destruction of beta-cells in murine type 1 diabetes. *Diabetes* 2010;59:1756–1764
- Jansen A, Homo-Delarche F, Hooijkaas H, Leenen PJ, Dardenne M, Drexhage HA. Immunohistochemical characterization of monocyte-macrophages and dendritic cells involved in the initiation of the insulinitis and beta-cell destruction in NOD mice. *Diabetes* 1994;43:667–675
- Furlan R, Cuomo C, Martino G. Animal models of multiple sclerosis. *Methods Mol Biol* 2009;549:157–173
- Kinne RW, Bräuer R, Stuhl Müller B, Palombo-Kinne E, Burmester GR. Macrophages in rheumatoid arthritis. *Arthritis Res* 2000;2:189–202
- Keir ME, Liang SC, Guleria I, et al. Tissue expression of PD-L1 mediates peripheral T cell tolerance. *J Exp Med* 2006;203:883–895
- Martin-Orozco N, Wang YH, Yagita H, Dong C. Cutting edge: programmed death (PD) ligand-1/PD-1 interaction is required for CD8+ T cell tolerance to tissue antigens. *J Immunol* 2006;177:8291–8295
- Zhang Y, Chung Y, Bishop C, et al. Regulation of T cell activation and tolerance by PDL2. *Proc Natl Acad Sci USA* 2006;103:11695–11700
- Shin T, Yoshimura K, Shin T, et al. In vivo costimulatory role of B7-DC in tuning T helper cell 1 and cytotoxic T lymphocyte responses. *J Exp Med* 2005;201:1531–1541
- Wällberg M, Harris RA. Co-infection with *Trypanosoma brucei brucei* prevents experimental autoimmune encephalomyelitis in DBA/1 mice through induction of suppressor APCs. *Int Immunol* 2005;17:721–728